Density Functional Study of the Electronic Structures of $[Co(NH_3)_5X]^{(3+n)+}$ Complexes. Insight into the Role of the 3d and 4s Orbitals in Metal−Ligand Interactions

Jerry C. C. Chan, Philip J. Wilson,† Steve C. F. Au-Yeung,* and Graham A. Webb†

Department of Chemistry, The Chinese University of Hong Kong, Shatin, New Territories, Hong Kong

Received: July 22, 1996; In Final Form: February 26, 1997[⊗]

The fundamental issue of the role of the Co 3d and 4s orbitals in the metal−ligand interactions of Co(III) complexes has been reexamined using density functional theory. It is suggested that the 3d and 4s orbitals take on a relative role depending on the symmetry-restricted covalency of a particular metal−ligand interaction. In all the $[Co(NH_3)_5X]^{(3+n)+}$ complexes studied in this work, the contribution of the Co 4s orbital in the metal−ligand bonding is predominant when the interaction is less covalent whereas the converse is true for the Co 3d orbitals. The covalency of the metal−ligand interactions in Co(III) complexes depends entirely on the different degrees of participation of the Co 3d orbitals. This result rationalizes the observed ^{59}Co NMR trends reported earlier on $[Co(NH_3)_5X]^{(3+n)+}$ complexes.

Introduction

Hexacoordinated Co(III) complexes are one of the most important classes of transition metal complexes because of their versatile coordination chemistry.[1] In a recent ^{59}Co NMR study of 37 diamagnetic hexacoordinated Co(III) complexes,[2] we have attempted to account for the large variation of the ^{59}Co shielding constants (*ca*. 12 000 ppm) by quantifying the contributions of the nephelauxetic effect and the d−d excitation energy (spectrochemical effect). We have demonstrated that the covalent characters of the metal−ligand interactions of hexacoordinated Co(III) complexes have a strong influence on the shielding constants of the central metal. Two correlation lines, viz. HH and HS, have been established for a series of $[Co(NH_3)_5X]^{(3+n)+}$ complexes (see Figure 1 in ref 2) when the ^{59}Co isotropic chemical shifts are correlated with the half-height line width and the averaged d−d excitation energies.[2] Accordingly, the HH and HS correlation lines manifest the hard metal−hard ligand and hard metal−soft ligand interactions, respectively. The difference in the *y*-intercepts (^{59}Co chemical shifts) of the HH and HS correlation lines is attributed to the contribution of bond covalency to the metal paramagnetic shielding (ca. 1200 ppm). Conceptually, the "nephelauxetic effect" and "bond covalency" are employed in the same sense as "charge transfer" in our previous study although the direction of electron flow is not known.[2] In order to obtain an in-depth understanding of the variations in the ^{59}Co shielding constants, which may provide insights into the chemical shielding properties for other transition metals with incomplete d-manifold, the observation of the HH and HS correlation lines reported earlier is suggested to be best interpreted by the changes in the metal electronic structures.

Gerloch has suggested[3] that for hexacoordinated complexes the 4s orbital of the metal atom plays an important role in the metal−ligand interaction for the first-row transition metal in *high oxidation states*. This rationale is based on a *larger radial maximum of the 4s orbital* in enhancing the overlap between the 4s and the ligand orbitals. In a previous self-consistent field (SCF) study,[4] Vanquickenborne *et al*. suggested that the bonding interactions of $[Co(CN)_6]^{3-}$ are basically dominated by the 3d orbitals because the 4s and 4p populations are relatively small. While the 3d orbitals may have more "inner" character and are thus unfavorable for bonding with ligand orbitals,[3] it is equally probable that the 3d orbital dominates the metal−ligand interaction because of the central field and/or symmetry-restricted covalency effects. It has also been suggested that, depending on the magnitude of the radial form of the "resultant" 3d orbitals, the valence shell of the first-row transition metal in a high oxidation state largely excludes the 3d functions;[3] however, its validity cannot be evaluated without invoking computational study.

Thus far, relatively few ab initio studies on these systems are reported. Most of the ab initio studies of Co(III) complexes are carried out at the Hartree−Fock (HF) level.[5] Although it is desirable to include electron correlation effects, post-Hartree−Fock studies involving transition metals are computationally very demanding.[6] It is now widely accepted that density functional theory (DFT) provides an efficient and reliable alternative to the post-Hartree−Fock methods.[7] The advancement in computational method and capacity enables a reexamination of these "classical" hexacoordinated Co(III) complexes which serve as good model systems for pursuing an understanding of the metal−ligand bonding of the first-row transition metals.

The primary purpose of this study is to investigate the role of the 3d, 4s, and 4p orbitals in the cobalt−ligand interaction and its relationship with the variation of the ^{59}Co shielding constant based on the results obtained from the Mayer bond order[8] (MBO) method, natural population analysis (NPA),[9] natural bond orbital[10] (NBO) method,[11] and Mulliken population analysis (MPA). In accordance with our previous ^{59}Co NMR study,[2] nine complexes from the series $[Co(NH_3)_5X]^{(3+n)+}$ (X = $\underline{N}O^-$, $\underline{S}CN^-$, $\underline{S}SO_3^{2-}$, Cl^-, $\underline{O}CO_2^{2-}$, $\underline{O}NO^-$, N_3^-, H_2O, $\underline{N}O_2^-$) were chosen for the present density functional study. All four bonding analysis methods are used to calculate the metal−ligand bonding properties and the results are compared to build an overall understanding of the metal−ligand interactions in $[Co(NH_3)_5X]^{(3+n)+}$. In particular, the Co−X covalence trend is established by the MBO method; the atomic populations are calculated using the NPA method whereas the NBO method is employed to give a detailed description of the role of the metal orbitals in the metal−ligand interactions. The results of the conventional MPA method are also compared with that of NBO to reveal the ambiguous role of the Co 4p orbitals.

* Author to whom correspondence should be addressed.
† Department of Chemistry, University of Surrey, Guilford, Surrey, England.
⊗ Abstract published in *Advance ACS Abstracts,* May 15, 1997.

S1089-5639(96)02201-3 CCC: $14.00 © 1997 American Chemical Society

Computational Details

Both the DFT modules of the Gaussian 94[12] and deMon-NMR1p0[13] packages were chosen for the investigation of the Co(III) compounds. The SCF densities obtained by the deMon-NMR1p0 package were analyzed by the MBO analysis method, while those calculated by the Gaussian 94 package were analyzed by the methods of NPA, NBO, and MPA.[14] NPA has been established as a good alternative method to the conventional MPA method for atomic charge calculation. The NBO analysis, which is intimately related to NPA, has been applied to a wide variety of systems including group IIIA metal oxides[15] and transition metal systems[16] such as hexamethyltungsten. Within the framework of NBO, electrons of a system are allocated to the lone pairs (LP), bond pairs (BP), core, and Rydberg orbitals in order to generate a Lewis structure. The populations of the corresponding antibonding orbitals (eg. LP*) serve as a non-Lewis correction to the calculated structure.

For the coordination complexes chosen in this study, a two-step procedure was adopted to calculate the metal−ligand bond covalency in a consistent way: (i) the principal Lewis structures of the complexes were calculated; (ii) the Lewis structures obtained were modified such that all the metal−ligand BPs were assigned as LPs residing on the ligand. That is, three lone pair electrons are allocated to the Co(III) metal ion (d^6) and the metal−ligand interactions are investigated by the second-order perturbative analysis (SOPA) of the ligand LP (donor) and metal LP* (acceptor) orbitals. The SOPA results are presented as a list of second-order interaction energies (E2) between donor and acceptor orbitals.

Among the many choices of the exchange-correlation (XC) functional available in Gaussian 94, B3LYP[17] has been shown to perform satisfactorily in general applications.[18,19] The B3LYP XC functional is a hybrid HF-DFT functional, and a detailed description of this functional can be found in the Gaussian manual.[20] The "pure" density functional Beck/Perdew[21] is employed in the calculation using deMon-NMR1p0 since the B3LYP XC functional is not available in this package. In general, the standard deMon auxiliary basis sets (5,5;5,5), (5,4;5,4), (5,2;5,2), and (2,3;2,3) were used for Co, (S, Cl), (C, N, O), and H atoms, respectively, in order to approximate the density and the XC potential.

The standard IGLO-II basis sets (311/1*), (51111/21111/1*), and (5111111/211111/11*) of Kutzelnigg et al.[22] were employed for the ligand atoms H, (C, N, O) and S, respectively. The Co TZVP basis set (61121111111/3111111111*/111111)[23] was constructed by uncontracting the TZV basis of Schäfer et al.[24] with two p-polarization functions added by Wachters.[25] The TZVP cobalt basis set has been tested by calculating the geometries of CoO and CoH.[26] The bond lengths obtained are comparable to those calculated by various post-Hartree−Fock methods.[26] The TZVP cobalt basis set and the IGLO-II ligand basis sets are considered to be balanced in adherence to Vanquickenborne's recipe.[27] That is, the $\Delta E/N$ values for the TZVP cobalt, IGLO-II carbon, IGLO-II nitrogen, IGLO-II oxygen, IGLO-II sulfur, and IGLO-II chlorine are, respectively, 3.997, 0.6554, 0.9063, 1.036, and 2.894 (in 10^{-3} hartrees).[28] Note that ΔE refers to the energy difference between the numerical HF energy of a given atom and the energy calculated by the basis set under consideration and N denotes the corresponding atomic number.

Experimental geometries from single-crystal X-ray crystallography studies were used and the literature references are given in Table 1. All the calculations were performed on the bare complexes with net charges ranging from +1 to +3. The coordinates of the hydrogen atoms which are missing in the reported structures were calculated by assuming a N−H bond length of 1.011 Å, a H−N−H bond angle of 106.7°, a O−H bond length of 0.941 Å, and a H−O−H bond angle of 105.4°.

TABLE 1: Mayer Bond Order Analysis of $[Co(NH_3)_5X]^{(3+n)+}$

X	Co−X	Co−NH_3^{eq} (averaged)	Co−NH_3^{ax}	structural reference
$\underline{N}O_2^-$	0.62	0.58	0.49	33
$\underline{O}NO^-$	0.62	0.58	0.55	34
$\underline{N}O^-$	1.09	0.53	0.35	35
$\underline{O}CO_2^{2-}$	0.76	0.53	0.46	36
$\underline{O}H_2$	0.47	0.63	0.68	37
$\underline{Cl}^-$	1.16	0.56	0.56	38
N_3^-	0.83	0.57	0.51	39
$\underline{S}CN^-$	0.99	0.58	0.53	40
$\underline{S}SO_3^{2-}$	1.15	0.54	0.45	41

Results and Discussion

Bond Covalency Analysis of $[Co(NH_3)_5X]^{(3+n)+}$. 1. Mayer Bond Order Analysis. The MBO bond index is a measure of the covalency between two interacting atoms.[29] This concept is related to the exchange part of the second-order density matrix and is readily applied to delocalized systems.[30] Although this bond index exhibits basis set dependence, the changes of the bond covalency in different systems are reflected satisfactorily in the changing trend of the bond indices. Unfortunately, the calculated Mayer bond order cannot be broken down to give the individual contributions arising from the various atomic orbitals. On the basis of the bond orders tabulated in Table 1, the trend of the Co−X covalency is

$$Cl^- > \underline{S}SO_3^{2-} > \underline{N}O^- > \underline{S}CN^- > N_3^- > \underline{O}CO_2^{2-} > NO_2^- > ONO^- > H_2O$$

In addition, the calculated bond orders of the Co−NH_3^{eq} (equatorial NH_3) and Co−NH_3^{ax} (axial NH_3) are given in the third and the fourth columns in Table 1. The results using single-crystal X-ray crystallography show that the *trans* effect is significant only in $[Co(NH_3)_5NO]^{2+}$. That is, the bond length of Co−NH_3^{ax} is significantly larger than that of Co−NH_3^{eq}. Although the difference in the bond orders of Co−NH_3^{eq} and Co−NH_3^{ax} vary from complex to complex, the established *trans* effect in $[Co(NH_3)_5NO]^{2+}$ is clearly revealed because of the substantially larger difference in the bond order.

2. Natural Population Analysis. The electron configuration of the Co as well as the natural charges of the ligand atoms in $[Co(NH_3)_5X]^{(3+n)+}$ are tabulated in Table 2. While the Co 3d (7.74−7.86) population varies noticeably in different complexes, the Co 4s (0.32−0.37) and 4p (0.01−0.03) populations remain essentially constant and are significantly smaller than the 3d population. Their magnitudes approximately agree with the Mulliken populations of $[Co(CN)_6]^{3-}$ (7.35, 0.45, and −0.04 for the 3d, 4s, and 4p orbitals, respectively) and $[Co(CN)_5(OH)]^{3-}$ (7.10, 0.37, and −0.07 for the 3d, 4s, and 4p orbitals, respectively).[4] The variation of the natural charge on Co is correlated with the natural population of the Co 3d orbitals (Figure 1). This trend indicates that the participation of the dσ orbitals in the coordination bond dominates the charge variation on Co, i.e. with increasing 3d electron donation to Co, the less positive the Co natural charge. While this finding demonstrates the prominent role of the Co 3d orbitals unequivocally, it is not a sufficient evidence to neglect the Co 4s and 4p orbitals in the Co−X interactions (vide infra).

The charge transferred from X to Co is estimated by comparing the NPA and formal charges of X. On the basis of

TABLE 2: Summary of the Electronic Configuration of Cobalt and Charge Distribution of $[Co(NH_3)_5X]^{(3+n)+}$ Calculated by the Natural Population Analysis

	electronic configuration of Co			charge distribution				total electrons donated
X	3d	4s	4p	Co	X	NH_3^{ax}	NH_3^{eq}	from X to Co[a]
$\underline{N}O_2^-$	7.80	0.34	0.02	0.83	−0.32	0.24	0.31	0.68
$\underline{O}NO^-$	7.75	0.35	0.03	0.87	−0.31	0.26	0.30[b] (1)	0.69
$\underline{N}O^-$	7.86	0.34	0.02	0.78	0.00	0.13	0.27	1.00
$\underline{O}CO_2^{2-}$	7.74	0.32	0.01	0.92	−1.18	0.19	0.26 (1)	0.82
$\underline{O}H_2$	7.66	0.34	0.01	0.99	0.20	0.39	0.36	0.20
$\underline{Cl}^-$	7.75	0.37	0.03	0.86	−0.40	0.27	0.32	0.60
N_3^-	7.76	0.34	0.02	0.88	−0.39	0.25	0.31 (1)	0.61
$\underline{S}CN^-$	7.84	0.37	0.02	0.78	−0.31	0.26	0.32 (1)	0.69
$\underline{S}SO_3^{2-}$	7.83	0.36	0.03	0.79	−1.08	0.18	0.28 (1)	0.91

[a] Estimated by comparing the charge of X and its formal charge. [b] The value in the parentheses indicates the variation of the charges of the four NH_3^{eq}.

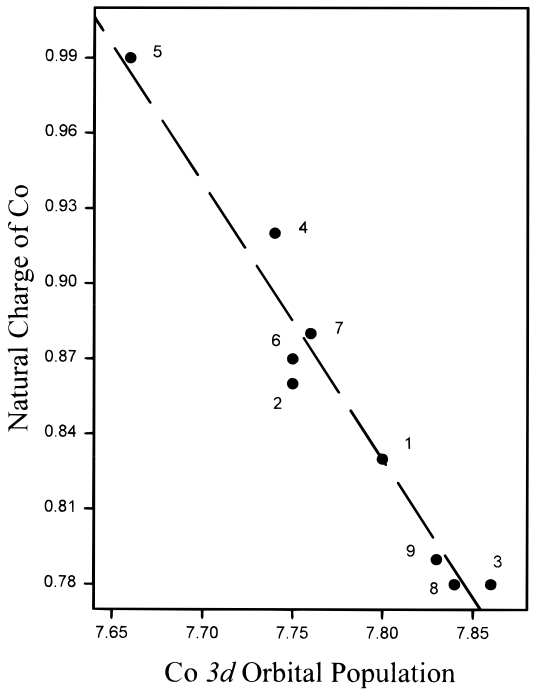

Figure 1. The natural charge of Co versus the Co 3d orbital population. The labels of the complexes correspond to those in Table 2.

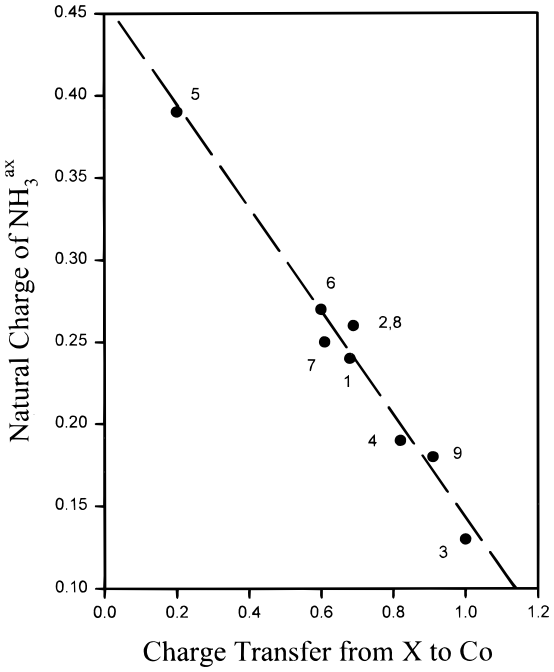

Figure 2. The natural charge of NH_3^{ax} versus the charge transfer from X to Co. The labels of the complexes correspond to those in Table 2.

the calculated results (the last column of Table 2), the covalency of the Co−X bond is ranked as follows:

$$\underline{N}O^- > \underline{S}SSO_3^{2-} > \underline{O}CO_2^{2-} > \underline{S}CN^- \approx \underline{O}NO^- \approx \underline{N}O_2^- > N_3^- > Cl^- \gg H_2O$$

This trend agrees reasonably well with that obtained by ranking the Mayer bond index except for $\underline{S}CN^-$, N_3^-, and Cl^-. The disagreement is not unexpected because the back-bonding effect cannot be accounted for in charge analysis. When the natural charges of NH_3^{ax} are plotted against the X to Co charge transfer (Figure 2), a satisfactory correlation line is obtained with a negative slope. A physical interpretation of the negative slope is identified with the *trans* effect of the X ligand. If the Co−X interaction is stronger, which is inferred by the X to Co charge transfer, the interaction of Co−NH_3^{ax} will be weaker and results in a less positive charge on NH_3^{ax}. On the basis of the projection of the data points on the correlation line of Figure 2, the trend of the *trans* effect is obtained:

$$\underline{N}O^- > \underline{S}SO_3^{2-} > \underline{O}CO_2^{2-} > \underline{N}O_2^- > \underline{S}CN^- \approx \underline{O}NO^- \approx N_3^- > Cl^- \gg H_2O$$

As expected, this trend agrees satisfactorily with that of the Co−X bond covalency. To summarize, the NPA results show that the Co 3d orbitals play a significant role in the valence shell of Co(III) and the *trans* effect is operating in the series of $[Co(NH_3)_5X]^{(3+n)+}$.

3. Natural Bond Orbital Analysis. According to the SOPA scheme, an E2 of 6 kcal/mol would roughly be equal to a charge transfer of 0.01 e when the charge transfer is favorable in one direction and the E2 is as small as a few kcal/mol.[10] Unfortunately, the calculated second-order perturbation energies of $[Co(NH_3)_5X]^{(3+n)+}$ (see Table 3) are extraordinarily high (83 to 783 kcal/mol), therefore the SOPA results are most likely less accurate. Since we are mainly interested in the *qualitative* picture of the cobalt−ligand interaction, we suggest that the SOPA scheme remains useful for studying the Co(3d,4s,4p)−ligand interactions. In Table 3, the second-order perturbation energies of ligand LP (donor) and cobalt LP* (acceptor) orbitals are summarized.

Since the E2 energies reveal the covalency of Co−X interaction, it is surprising at first sight to find that the calculated E2 energies of N_3^-LP/CoLP*, $\underline{S}CN^-$LP/Co LP*, and SSO_3^{2-}/Co LP* are comparable to that of $\underline{O}H_2$LP/Co LP*. While the E2 energy of the orbital pair X LP/Co LP* is identified with the charge transfer from ligands to cobalt, the E2 of Co LP/X

TABLE 3: Second-Order Perturbative Analysis of Donor LP/Acceptor LP* Orbitals of $[Co(NH_3)_5X]^{(3+n)+}$

	X LP/Co LP*			N^{eq} LP/Co LP*			N^{aX} LP/Co LP*		
X	E2 (kcal/mol)	contribn (%) Co 3d	contribn (%) Co 4s	averaged E2 (kcal/mol)	contribn (%) Co 3d	contribn (%) Co 4s	E2 (kcal/mol)	contribn (%) Co 3d	contribn (%) Co 4s
$\underline{N}O_2^-$	144	61	39	102	43	57	105	51	49
$\underline{O}NO^-$	123	61	39	102	44	56	96	41	59
$\underline{N}O^-$	324	81	19	96	40	60	51	32	68
$\underline{O}CO_2^{2-}$	151	64	36	96	43	57	87	38	62
$\underline{O}H_2$	78	32	68	138	58	42	121	47	53
$\underline{Cl}^-$	403	79	21	108	41	59	113	55	45
N_3^-	84	23	77	102	43	57	106	49	51
	(325)[a]	100	0						
$\underline{S}CN^-$	92	0	100	114	42	58	113	55	45
	(783)[a]	100	0						
$\underline{S}SO_3^{2-}$	83	0	100	102	40	60	85	49	51
	(654)[a]	100	0						

[a] The figure in the parentheses is the E2 energy of Co LP*/X LP which reveals the extent of electron back-donation.

LP* reveals the extent of charge transfer from cobalt to ligands (electron back-donation). Although the E2 energies of X LP/Co LP* for $[Co(NH_3)_5N_3]^{2+}$, $[Co(NH_3)_5SCN]^{2+}$, and $[Co(NH_3)_5S_2O_3]^+$ are surprisingly small, the calculated E2 energies of Co LP*/X LP are 325, 783, and 654 kcal/mol for $[Co(NH_3)_5N_3]^{2+}$, $[Co(NH_3)_5SCN]^{2+}$, and $[Co(NH_3)_5S_2O_3]^+$, respectively. These E2 energies show that charge transfer from Co to X is important in $[Co(NH_3)_5N_3]^{2+}$, $[Co(NH_3)_5SCN]^{2+}$, and $[Co(NH_3)_5S_2O_3]^+$. It seems that the covalency of Co−N_3, Co−SCN, and Co−S_2O_3 are mainly constituted of Co to X back-bonding effect. Since the occupation number of Co LP*s are relatively small for these three complexes (0.98−1.12), a direct comparison of them with the other complexes is likely meaningless. Therefore, the SOPA results of $[Co(NH_3)_5N_3]^{2+}$, $[Co(NH_3)_5SCN]^{2+}$, and $[Co(NH_3)_5S_2O_3]^+$ provide a *qualitative* description of their bonding environment. That is, the X ligand donates electrons to the Co 4s orbital and accepts electrons from the Co 3d orbitals, and the Co−X covalency in these complexes mainly originates from the electron back-donation from Co to X. Note that Co−Cl back-bonding effect is not found for $[Co(NH_3)_5Cl]^{2+}$. Without considering $[Co(NH_3)_5N_3]^{2+}$, $[Co(NH_3)_5SCN]^{2+}$, and $[Co(NH_3)_5S_2O_3]^+$, the covalency of the Co−X bond is ranked as follows based on the calculated E2 energies:

$$Cl^- > \underline{N}O^- > \underline{O}CO_2^{2-} \approx \underline{N}O_2^- > \underline{O}NO^- > H_2O$$

This sequence agrees favorably with that obtained from Mayer bond order index. The calculated E2 for N^{ax} LP/Co LP* orbitals is smaller than that of N^{eq} LP/Co LP* for $[Co(NH_3)_5NO]^{2+}$, which is consistent with the rule of thumb that the longer the bond length the weaker the bond strength for the same type of bonding. Among these complexes, the Co 4s orbital dominates the Co−NH_3^{eq} interaction whereas the Co 3d orbital dominates the Co−X interaction except for $[Co(NH_3)_5H_2O]^{3+}$. The contribution from the Co 4p orbitals remains negligible in all cases.

The above results indicate that the importance of the Co 3d orbital in some of the Co−X interactions is derived from the symmetry-restricted covalency. For $[Co(NH_3)_5Cl]^{2+}$, the covalency of the Co−Cl bond is so large that the electrons donated from Cl to Co cause an expansion of the symmetry-adapted Co 3d orbital(s) such that the overlap of these particular Co 3d orbital(s) and the Cl donor orbital(s) dominate the Co−Cl interaction. On the other hand, the covalency of Co−NH_3^{eq} is not enhanced by the charge transfer from Cl to Co and thus the Co 4s orbital remains dominating for the Co−NH_3^{eq} interaction. The same rationalization is applicable to other complexes except $[Co(NH_3)_5H_2O]^{3+}$. The interchanged role of the Co 4s and 3d orbitals in $[Co(NH_3)_5H_2O]^{3+}$ shows that the covalency of Co−H_2O is smaller than that of Co−NH_3 and the enhancement of Co−NH_3 covalency is accompanied by the more active participation of the Co 3d orbitals.

In short, the calculated results demonstrate that *the participation of the Co* 4s *orbital will be predominant in a less covalent metal−ligand bond whereas the Co* 3d *orbital will play a more significant role in a covalent environment*. This finding clarifies unequivocally the origin of the HH and HS correlations of Co(III) complexes.[2] Since the s electrons do not contribute to paramagnetic shielding, the HH and HS correlation lines established for $[Co(NH_3)_5X]^{(3+n)+}$ are mainly the result of the different degrees of metal−ligand charge transfer involving the active participation of 3d orbitals. Note that both experimental[2] (the HH and HS correlation lines) and the calculated results confirm that the conventional ligand field description for Co(III) complexes where it has been stated that the bonding scheme of the first-row transition metal is solely carried by the 3d electrons (*without considering* 4s *electrons*),[4] may not be fully justified. On the other hand, it is also invalid to exclude the 3d orbitals from the valence shells of transition metals at high oxidation states.[3]

4. Mulliken Population Analysis. In Table 4, the Mulliken gross populations of Co in each complex are tabulated. While the order of the magnitude of the Mulliken gross population of the Co 3d and 4s orbitals agree reasonably well with the results obtained from NPA analysis, there is a significant amount of Co 4p population found in the MPA calculation. Although MPA has been previously criticized for allocating too much electron density to the metal s and p orbitals,[31] the issue concerning whether the metal NPA "valence" space contains p orbitals remains unresolved. It should be noted that the involvement of 4p orbitals in the metal NPA "valence" may increase the natural 4p population significantly.[32]

From the population matrix of the MPA, the overlap population between Co and the ligating atoms are broken down into the individual overlap contributions from orbitals with different angular momenta (Table 5). In stark contrast to the conclusion reached from the NBO results, the Co 4p orbitals play an important role in the metal−ligand interaction. As a result, the Co 4p orbitals dominate the valence of Co in the Co−X bonding of $[Co(NH_3)_5SCN]^{2+}$, $[Co(NH_3)_5Cl]^{2+}$, and $[Co(NH_3)_5S_2O_3]^+$; the 4s orbital dominates the valence of Co in the Co−X bonding $[Co(NH_3)_5N_3]^{2+}$ and $[Co(NH_3)_5CO_3]^+$; and the 3d orbitals dominate the valence of Co in the Co−NO_2 bonding of $[Co(NH_3)_5NO_2]^{2+}$. For the remaining complexes

TABLE 4: Summary of the Electronic Configuration of Cobalt and Charge Distribution of $[Co(NH_3)_5X]^{(3+n)+}$ Calculated by the Mulliken Population Analysis

	electronic configuration of Co			charge distribution			
X	3d	4s	4p	Co	X	NH_3^{ax}	NH_3^{eq}
$\underline{N}O_2^-$	7.43	0.40	0.70	0.46	−0.21	0.30	0.36
$\underline{O}NO^-$	7.43	0.46	0.70	0.40	−0.14	0.30	0.36 (1)
$\underline{N}O^-$	7.48	0.42	0.60	0.51	0.04	0.19	0.32 (1)
$\underline{O}CO_2^{2-}$	7.41	0.37	0.61	0.61	−0.97	0.23	0.29 (1)
$\underline{O}H_2$	7.34	0.39	0.68	0.58	0.25	0.46	0.43
$\underline{Cl}^-$	7.41	0.35	0.82	0.42	−0.22	0.33	0.37 (1)
N_3^-	7.37	0.41	0.69	0.54	−0.24	0.30	0.35 (2)
$\underline{S}CN^-$	7.42	0.44	0.74	0.41	−0.15	0.31	0.36
$\underline{S}SO_3^{2-}$	7.43	0.44	0.76	0.37	−0.78	0.22	0.30

TABLE 5: Summary of the Overlap Population of $[Co(NH_3)_5X]^{(3+n)+}$ Calculated by the Mulliken Population Analysis

	Co−X						difference between
X	total	Co 3d[a]	Co 4s[a]	Co 4p[a]	$Co-NH_3^{eq}$ (averaged)	$Co-NH_3^{ax}$	$Co-NH_3^{eq}$ and $Co-NH_3^{ax}$
$\underline{N}O_2^-$	0.31	57	15	28	0.36	0.31	0.05
$\underline{O}NO^-$	0.32	37	40	23	0.32	0.28	0.04
$\underline{N}O^-$	0.44	39	18	43	0.32	0.26	0.06
$\underline{O}CO_2^{2-}$	0.45	16	57	27	0.29	0.26	0.03
$\underline{O}H_2$	0.33	24	28	48	0.38	0.40	−0.02
$\underline{Cl}^-$	0.80	17	16	67	0.29	0.35	−0.06
N_3^-	0.68	21	59	20	0.32	0.29	0.03
$\underline{S}CN^-$	0.73	19	22	59	0.33	0.31	0.02
$\underline{S}SO_3^{2-}$	0.74	18	15	67	0.30	0.28	0.02

[a] Distribution percentages.

($[Co(NH_3)_5H_2O]^{2+}$, $[Co(NH_3)_5ONO]^{2+}$, and $[Co(NH_3)_5NO]^{2+}$), the Co 3d, 4s, and 4p orbitals all contribute to the Co−X interaction.

The overlap populations of $Co-NH_3^{eq}$ and $Co-NH_3^{ax}$ (the sixth and seventh columns in Table 5) fail to reproduce the established *trans* effects in $[Co(NH_3)_5NO]^{2+}$. Nevertheless, the larger variation in the Co−X overlap population may provide a more reasonable measure in ranking the metal−ligand bond covalency. A detailed examination of the overlap population reveals the Co−X bonding covalency trend as

$$Cl^- > \underline{S}SO_3^{2-} \approx \underline{S}CN^- > N_3 > \underline{O}CO_2 \approx \underline{N}O^- > H_2O \approx ONO^- \approx NO^-_2$$

The sequence essentially agrees with that obtained from MBO analysis except for the position of NO^-. A comparison of NBO and MPA results shows that the role of the Co 4p orbitals in the metal−ligand interactions are not clearly known.

Conclusion

The origin of the HH and HS correlation lines observed in the analysis of ^{59}Co chemical shifts has shown to be the consequence of the active participation of the 3d orbital in the metal−ligand charge transfer. In contrast to the suggestion by Vanquickenborne,[4] the NBO analysis demonstrates that the relatively small Co 4s orbital population does not necessarily imply a negligible contribution of the Co 4s orbital to the metal−ligand interactions. We suggest that the 4s and 3d orbitals take on a relative role depending on the symmetry-restricted covalency of a particular metal−ligand interaction. In all the $[Co(NH_3)_5X]^{(3+n)+}$ complexes studied in this work, the contribution of the Co 4s orbital in metal−ligand bonding is predominant when the interaction is less covalent. The converse is true for the Co 3d orbitals. On the basis of the fact that the population of the Co 4s orbitals (0.32−0.36) does not vary significantly compared with that of the Co 3d orbitals (7.72−7.83), we conclude that the bonding picture of the metal−ligand interaction in Co(III) complexes depends to a greater extent on the different degrees of participation of the Co 3d orbitals. Unfortunately, the role of the Co 4p orbitals in the Co−ligand interactions cannot be shown unambiguously because of the intrinsic limitations in the NPA, MPA, NBO, and MBO methods. While Gerloch correctly emphasizes the role of the metal 4s orbital in the bonding of the first-row transition metals in high oxidation states, our calculations show that the 3d orbitals should not be excluded from the metal valency.

Acknowledgment. This research was supported by a RGC Earmarked Grant (CUHK 312/94P). The authors express their sincere gratitude to Profs. F. Weinhold, I. Mayer, J. Badenhoop, M. Kaupp, and E. Glendening for their prompt reply to our enquiries. The comments of the referees are also gratefully acknowledge.

References and Notes

(1) Buckingham, D. A.; Clark, C. R. In *Comprehensive Coordination Chemistry, The Synthesis, Reactions, Properties and Applications of Coordination Compounds, Volume 4*; Wilkinson, G., Gillard, R. D.; McCleverty, J. A., Eds.; Pergamon Press: Oxford, 1987.

(2) Chan, J. C. C.; Au-Yeng, S. C. F. *J. Chem. Soc. Faraday Trans.* **1996**, *92* (7), 1121.

(3) Gerloch, M. *Coord. Chem. Rev.* **1990**, *99*, 117.

(4) Vanquickenborne, L. G.; Hendrickx, M.; Hyla-Kryspin, I.; Haspeslagh, L. *Inorg. Chem.* **1986**, *25*, 885.

(5) (a) Noell, J. O.; Morokuma, K. *Inorg. Chem.* **1979**, *18*, 2774. (b) Vanquickenborne, L. G.; Hendrickx, M.; Postelmans, D.; Hyla-Kryspin, I.; Pierloot, K. *Inorg. Chem.* **1988**, *27*, 900. (c) Vanquickenborne, L. G.; Hendrickx, M.; Hyla-Kryspin, I. *Inorg. Chem.* **1989**, *28*, 770.

(6) Ernst, M. C.; Royer, D. J. *Inorg. Chem.* **1993**, *32*, 1226.

(7) *Density Function Methods in Chemistry*; Labanowski, J. K., Andzelm, J. W., Eds.; Springer: Berlin, 1991.

(8) Mayer, I. *Int. J. Quantum Chem.* **1986**, *29*, 477 and references therein.

(9) Reed, A. E.; Weinstock, R. B.; Weinhold, F. *J. Chem. Phys.* **1985**, *83*, 735.

(10) Reed, A. E.; Curtiss, L. A.; Weinhold, F. *Chem. Rev.* **1988**, *88*, 899 and references therein.

(11) NBO version 3.1 was employed in the analysis.

(12) Frisch, M. J.; Trucks, G. W.; Schlegel, H. B.; Gill, P. M. W.; Johnson, B. G.; Robb, M. A.; Cheeseman, J. R.; Keith, T.; Petersson, G.

A.; Montgomery, J. A.; Raghavachari, K.; Al-Laham, M. A.; Zakrzewski, V. G.; Ortiz, J. V.; Foresman, J. B.; Cioslowski, J.; Stefanov, B. B.; Nanayakkara, A.; Challacombe, M.; Peng, C. Y.; Ayala, P. Y.; Chen, W.; Wong, M. W.; Andres, J. L.; Replogle, E. S.; Gomperts, R.; Martin, R. L.; Fox, D. J.; Binkley, J. S.; Defrees, D. J.; Baker, J.; Stewart, J. P.; Head-Gordon, M.; Gonzalez, C.; Pople, J. A. *Gaussian 94, Revision B.2*; Gaussian Inc.: Pittsburgh, PA, 1995.

(13) (a) St-Amant, A.; Salahub, D. R. *Chem. Phys. Lett.* **1990**, *169*, 387. (b) Salahub, D. R.; Fournier, R.; Mlynarski, P.; Papai, I.; St-Amant, A.; Ushio, J. In *Density Functional Methods in Chemistry*; Labanowski, J., Andzelm, J., Eds.; Springer: New York, 1991. (c) St-Amant, A. Ph.D. Thesis, Université de Montréal, Montréal, Canada, 1992. (d) Godbout, N.; Salahub, D. R.; Andzelm, J.; Wimmer, E. *Can. J. Chem.* **1992**, *70*, 560.

(14) Since the Kohn−Sham orbitals are considered from a formal theoretical viewpoint as having no physical meaning except in giving the exact density, it is not totally justifiable to apply the wave functions-based analysis schemes to Kohn−Sham orbitals. In practice, however, the KS orbitals can be considered as reasonable approximations to the Hartree−Fock ones. Our work presents a positive argument to this assumption.

(15) Nemukhin, A. V.; Weinhold, F. *J. Chem. Phys.* **1992**, *97*, 3420. Nemukhin, A. V.; Weinhold, F. *J. Chem. Phys.* **1993**, *98*, 1329.

(16) (a) Lledos, A.; Suades, J.; Alvarez-Larena, A.; Piniella, J. F. *Organometallics* **1995**, *14*, 1053. (b) Kaupp, M. *J. Am. Chem. Soc.* **1996**, *118*, 3018.

(17) (a) Becke, A. D. *J. Chem. Phys.* **1993**, *98*, 5648. (b) Lee, C.; Yang, W.; Parr, R. G. *Phys. Rev. B* **1988**, *37*, 785. (c) Miehlich, B.; Savin, A.; Stoll, H.; Preuss, H. *Chem. Phys. Lett.* **1989**, *157*, 200.

(18) Baker, J.; Muir, M.; Andzelm, J. *J. Chem. Phys.* **1995**, *102*, 2063.

(19) Hay, P. J. *J. Phys. Chem.* **1996**, *100*, 5.

(20) Frisch, M. J.; Frisch, A.; Foresman, J. B. *Gaussian 94 User's Reference*; Gaussian Inc.: Pittsburg, PA, 1995.

(21) (a) Becke, A. D. *Phys. Rev. A* **1988**, *38*, 3098. (b) Perdew, J. P. *Phys. Rev. B* **1986**, *33*, 8822.

(22) Kutzelnigg, W.; Fleischer, U.; Schindler, M. *NMR: Basic Princ. Prog.* **1990**, *23*, 165.

(23) Malkin, V. G.; Malkina, O. L. Unpublished result.

(24) Schäfer, A.; Horn, H.; Ahlrichs, R. *J. Chem. Phys.* **1992**, *97*, 2571.

(25) Wachters, A. J. H. *J. Chem. Phys.* **1970**, *52*, 1033.

(26) Chan, J. C. C.; Au-Yeung, S. C. F.; Wilson, P. J.; Webb, G. A. *J. Mol. Struct. (THEOCHEM)* **1996**, *365*, 125.

(27) Vanquickenborne, L. G.; Verhulst, J.; Coussens, B.; Hendrickx, M.; Pierloot, K. *J. Mol. Struct. (THEOCHEM)* **1987**, *153*, 227.

(28) Froese Fischer, C. *The Hartree-Fock Method for Atoms. A Numerical Approach*; Wiley: New York, 1977.

(29) Mayer, I. *Theor. Chim. Acta* **1985**, *67*, 315.

(30) Mayr, I. Private communication.

(31) Harris, H. A.; Kanis, D. R.; Dahl, L. F. *J. Am. Chem. Soc.* **1991**, *113*, 8602.

(32) Maseras, F.; Morokuma, K. *Chem. Phys. Lett.* **1992**, *195*, 500.

(33) Cotton, F. A.; Edwards, W. T. *Acta Crystallogr.* **1968**, *B24*, 474.

(34) Grenthe, I.; Nordin, E. *Inorg. Chem.* **1979**, *18* (7), 1869.

(35) Pratt, C. S.; Coyle, B. A.; Ibers, J. A. *J. Chem. Soc.* **1971**, *A*, 2146.

(36) Freeman, H. C.; Robinson, G. *J. Chem. Soc.* **1965**, 3194.

(37) Solans, X.; Miravitlles, C.; Germain, G.; Declercq, J. P. *Acta Crystallogr.* **1979**, *B35*, 2181.

(38) Messmer, G. G.; Amma, E. L. *Acta Crystallogr.* **1968**, *B24*, 417.

(39) Palenik, G. J. *Acta Crystallogr.* **1964**, *17*, 360.

(40) Snow, M. R.; Boomsma, R. F. *Acta Crystallogr.* **1972**, *B28*, 1908.

(41) Restivo, R. J.; Ferguson, G.; Balahura, R. J. *Inorg. Chem.* **1977**, *16*, 167.